https://doi.org/10.1093/plphys/kiac148 PLANT PHYSIOLOGY 2022: 00: 1–12

Plant Physiology®

Research Report

Extracellular ATP plays an important role in systemic wound response activation

Ronald J. Myers Jr [1], Yosef Fichman [1], Gary Stacey [1], and Ron Mittler [1,*,†]

1 The Division of Plant Sciences Technology, Interdisciplinary Plant Group, College of Agriculture, Food and Natural Resources, Christopher S. Bond Life Sciences Center, University of Missouri, Columbia, Missouri 65201, USA

*Author for correspondence: mittlerr@missouri.edu
†Senior author.

R.J.M. and Y.F. performed the research. R.M. supervised the research and provided laboratory infrastructure and funding. R.M. and G.S. provided resources. R.J.M., Y.F., G.S., and R.M. wrote the manuscript and prepared the figures. All authors read and approved the final version of the manuscript.
The author responsible for distribution of materials integral to the findings presented in this article in accordance with the policy described in the Instructions for Authors (https://academic.oup.com/plphys/pages/general-instructions) is: Ron Mittler (mittlerr@missouri.edu).

Abstract

Mechanical wounding occurs in plants during biotic or abiotic stresses and is associated with the activation of long-distance signaling pathways that trigger wound responses in systemic tissues. Among the different systemic signals activated by wounding are electric signals, calcium, hydraulic, and reactive oxygen species (ROS) waves. The release of glutamate (Glu) from cells at the wounded tissues was recently proposed to trigger systemic signal transduction pathways via GLU-LIKE RECEPTORs (GLRs). However, the role of another important compound released from cells during wounding (extracellular ATP [eATP]) in triggering systemic responses is not clear. Here, we show in Arabidopsis (*Arabidopsis thaliana*) that wounding results in the accumulation of nanomolar levels of eATP and that these levels are sufficient to trigger the systemic ROS wave. We further show that the triggering of the ROS wave by eATP during wounding requires the PURINORECEPTOR 2 KINASE (P2K) receptor. Application of eATP to unwounded leaves triggered the ROS wave, and the activation of the ROS wave by wounding or eATP application was suppressed in mutants deficient in P2Ks (e.g. *p2k1-3*, *p2k2*, and *p2k1-3p2k2*). In addition, expression of systemic wound response (SWR) transcripts was suppressed in mutants deficient in P2Ks during wounding. Interestingly, the effect of Glu and eATP application on ROS wave activation was not additive, suggesting that these two compounds function in the same pathway to trigger the ROS wave. Our findings reveal that in addition to sensing Glu via GLRs, eATP sensed by P2Ks plays a key role in the triggering of SWRs in plants.

Introduction

Mechanical wounding is associated in plant cells with the disruption of cellular integrity and the breakdown of different membrane structures (Farmer et al., 2020; Ikeuchi et al., 2020; Vega-Muñoz et al., 2020). In many cases, this disruption results in the rapid and uncontrolled partitioning of cellular compounds, membrane depolarization, altered pH levels, and/or formation of reactive oxygen species (ROS; Farmer and Goossens, 2019; Shao et al., 2020; Vega-Muñoz et al., 2020). Mechanical wounding can occur in plants during herbivory, wind damage, pathogen infection, or even as part of different abiotic stresses such as severe drought, freezing, heat, or salt stresses that cause the collapse of different subcellular structures. In some cases, wounding is an early response to stress (e.g. during herbivory), while in others (e.g. following the activation of programmed cell death in response to pathogen attack) it could be a late event. One of the key processes associated with wounding is the disruption of plasma membrane (PM) integrity and the

Received January 05, 2022. Accepted March 06, 2022. Advance access publication March 28, 2022
© American Society of Plant Biologists 2022. All rights reserved. For permissions, please email: journals.permissions@oup.com

Downloaded from https://academic.oup.com/plphys/advance-article/doi/10.1093/plphys/kiac148/6555012 by University of Missouri-Columbia user on 06 June 2022

release of different cellular compounds such as the amino acid glutamate (Glu), or the nucleotide adenosine triphosphate (ATP) that becomes extracellular ATP (eATP; Roux, 2014; Toyota et al., 2018; Shao et al., 2020). Some of the compounds released from cells during wounding are thought to be sensed by different receptors (e.g. the PURINORECEPTOR 2 KINASE [P2K] that senses eATP; Choi et al., 2014; Chen et al., 2017; Pham et al., 2020), and/or channels (e.g. the Glu-like channels GLU-LIKE RECEPTORs GLR3.3 and GLR3.6 that sense Glu; Mousavi et al., 2013; Toyota et al., 2018; Shao et al., 2020; Tian et al., 2020) and trigger wound-induced signal transduction pathways (Monshausen et al., 2009; Tian et al., 2020; Moore et al., 2021). Wound-induced depolarization of the PM is also thought to alter the activity of additional channels and trigger further downstream signaling pathways (Nguyen et al., 2018; Farmer et al., 2020; Vega-Muñoz et al., 2020; Duong et al., 2021). In addition, the plant hormone jasmonic acid (JA) is produced at very high levels following the disruption of membranes and the oxidation of different fatty acids (Tripathi et al., 2017; Farmer and Goossens, 2019). JA, as well as other plant hormones, such as ethylene and salicylic acid, are also known to play a key role in the activation of wound-induced signaling.

In addition to triggering transcriptomic, metabolic, physiological, and/or proteomic responses at the tissues directly subjected to wounding (i.e. the wounded cells themselves, or cells neighboring the wounded cells; will be referred to here as "local tissue"), wounding is also accompanied by the triggering of systemic signal transduction pathways that activate wound-associated response mechanisms in tissues that have not been directly subjected to wounding (will be referred to here as "systemic tissue"). This process is termed systemic wound response (SWR) and is thought to enhance the overall resistance of plants to herbivory attack or other wound-related stresses (Walker-Simmons et al., 1984). Systemic signals thought to be involved in SWR include rapid changes in membrane potential (electric signals), calcium waves, ROS waves, hydraulic waves, and hormones such as JA (that can also function as volatiles; e.g. methyl JA), as well as other hormones and metabolites (e.g. Farmer et al., 2014, 2020; Tripathi et al., 2017; Nguyen et al., 2018; Toyota et al., 2018; Fichman et al., 2019; Matthus et al., 2020; Shao et al., 2020; Fichman and Mittler, 2021).

The release of Glu from wounded cells, as well as local changes in pH, were recently proposed to play a key role in triggering SWRs by activating GLRs and initiating the systemic calcium wave (Toyota et al., 2018; Shao et al., 2020). In addition to the calcium wave, GLRs were previously shown to be required for the activation of systemic electric waves during wounding (Mousavi et al., 2013; Nguyen et al., 2018). A recent study showed that GLRs are also required for triggering the ROS wave during wounding (Fichman and Mittler, 2021). In contrast to Glu, the role of eATP in triggering systemic responses to wounding is not established. eATP was shown to trigger local ROS production during wounding following the sensing of eATP by the eATP receptor P2K that phosphorylates and activates the RESPIRATORY BURST OXIDASE HOMOLOG D (RBOHD) protein (Chen et al., 2017). A recent study has also shown that eATP is activating calcium signaling in cells via CYCLIC NUCLEOTIDE GATED ION CHANNEL2 (CNGC2) and CNGC2 (Duong et al., 2021; Wang et al., 2022), and this process could also activate the calcium and ROS waves (Matthus et al., 2020).

The ROS wave is an auto-propagating cell-to-cell systemic signaling pathway triggered in plants in response to wounding and many different biotic and abiotic stresses (e.g. Fichman et al., 2019; Fichman and Mittler, 2020; Zandalinas et al., 2020a, 2020b; Zandalinas and Mittler, 2021). It is dependent on the function of RBOHD and can travel in a cell-to-cell fashion over long distances from its site of initiation to the entire plant within minutes (Miller et al., 2009; Fichman et al., 2019; Fichman and Mittler, 2020). A recent study showed that the activation of the ROS wave in plants during wounding does not occur in mutants deficient in GLR (i.e. the *glr3.3glr3.6* double mutant), RBOHD (*rbohD*), or plasmodesmata (PD) functions (i.e. mutations in PD-LOCALIZED PROTEIN 5; *pdlp5;* Fichman and Mittler, 2021). However, the role of eATP in triggering the ROS wave and other systemic responses during wounding is not clear.

Because RBOHD plays a critical role in eATP-induced ROS formation during wounding (Chen et al., 2017), as well as in triggering and propagating the ROS wave (Miller et al., 2009; Fichman and Mittler, 2020), we used the whole-plant imaging method we developed (Fichman et al., 2019; Zandalinas et al., 2020a, 2020b; Fichman and Mittler, 2021; Zandalinas and Mittler, 2021) to elucidate the role of eATP in the wound-induced ROS wave response. Here, we reveal that eATP that accumulates in wounded leaves and is sensed by P2K is required for the activation of the ROS wave during wounding. eATP application to unwounded leaves triggered the ROS wave, and the activation of the ROS wave was suppressed in mutants deficient in P2K (i.e. *p2k1-3*, *p2k2*, and *p2k1-3p2k2*). In addition, the expression of several SWR transcripts was suppressed in mutants deficient in P2K during wounding. Our findings reveal that in addition to sensing Glu via GLRs, eATP sensed by P2Ks is playing a key role in triggering the SWR of plants.

Results and discussion

Whole-plant live imaging of eATP accumulation in plants following wounding

eATP was previously imaged following wounding of plant tissues using a combination of luciferase and luciferin that produces light in the presence of ATP (e.g. Kim et al., 2006; Roux, 2014). These measurements were, however, restricted to cells and tissues and conducted using different microscopy platforms. To image eATP accumulation following wounding in whole Arabidopsis (*Arabidopsis thaliana*) plants grown in soil, we used the same imaging platform we previously used for live imaging of ROS in whole plants in response to different stresses/treatments (i.e. the IVIS Lumina S5 platform; Fichman et al., 2019). We applied a mixture of

Downloaded from https://academic.oup.com/plphys/advance-article/doi/10.1093/plphys/kiac148/6555012 by University of Missouri-Columbia user on 06 June 2022

luciferin and luciferase to plants and imaged light emission from plants following wounding. As shown in Figure 1, A and B, we first generated a calibration curve for ATP and then used this curve to measure the levels of ATP released from cells within the first 5 min following wounding. This analysis revealed that~35 nM of ATP can be detected on the surface of leaves 5 min following wounding (Figure 1, A and B). This amount is much lower than previous findings (about 40 1M; Song et al., 2006), potentially due to the higher sensitivity of the equipment used in this study. Using the whole-plant ATP imaging method we developed (Figure 1, A and B), we then determined for how long ATP levels would persist on a leaf following wounding. As shown in Figure 1C, wounding of a single leaf of Arabidopsis resulted in the rapid accumulation of eATP that began to subside at about 20 min following wounding. Systemic accumulation of eATP in nonwounded leaves of treated plants or in unwounded plants was not detected. The findings

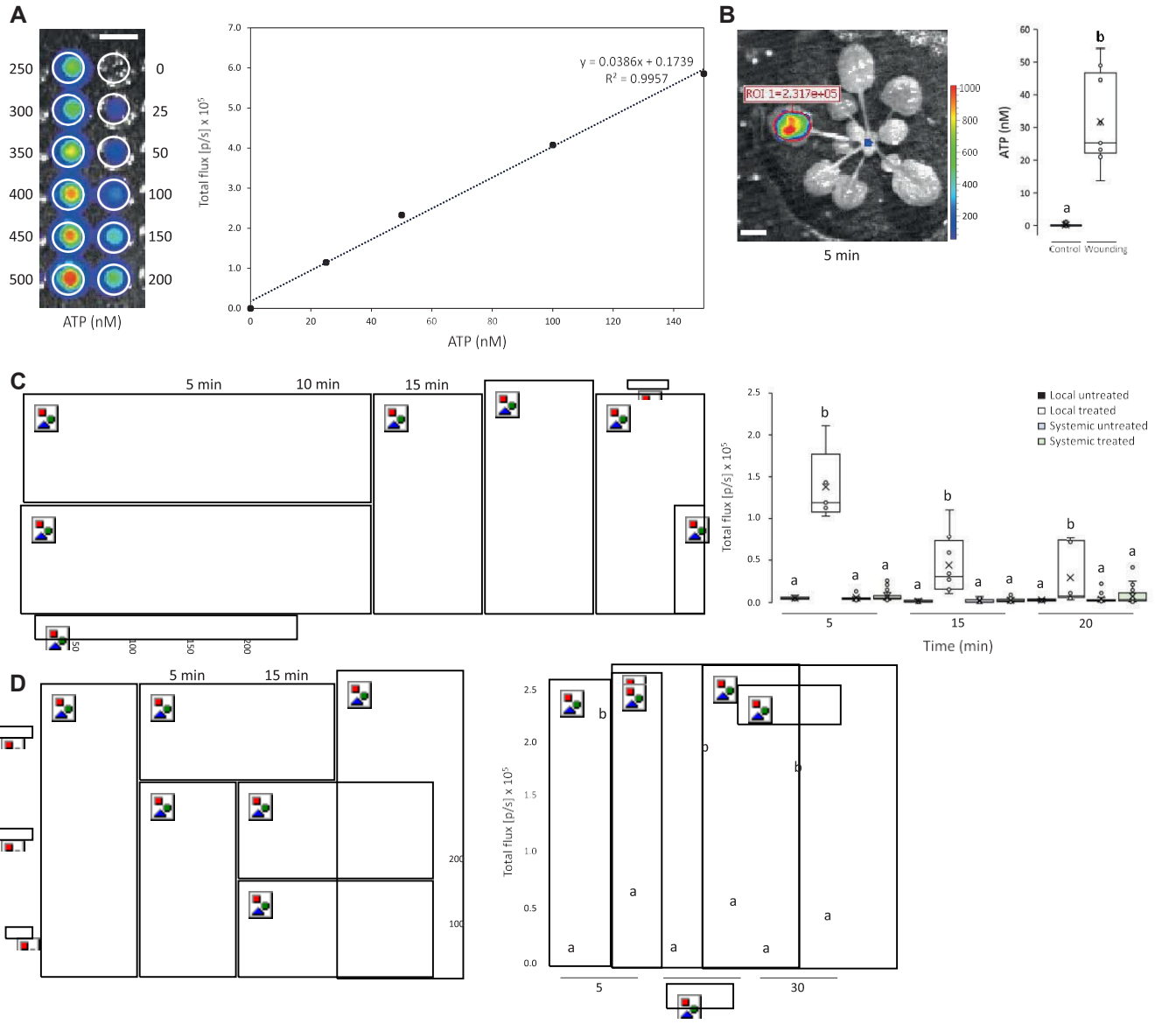

Figure 1 Whole-plant live imaging of eATP accumulation following wounding. A, A representative calibration curve generated to measure ATP levels using the IVIS Illumina S5 platform. B, Quantification of ATP levels (indicated by luciferase activity) in a wounded Arabidopsis leaf 5 min following wounding. C, Representative time-lapse images of whole plant eATP levels in Arabidopsis plants subjected to wounding on a single leaf (local; L), along with statistical analysis of eATP levels in L and systemic (S) leaves of wounded (on leaf L) and unwounded plants at 5-, 15- and 20-min following wounding. D, Representative time-lapse images of luciferase activity following the application of 0, 300, or 600 1M of ATP to a single leaf (L), along with statistical analysis of eATP levels in leaf L at 5-, 15-, and 30-min following ATP application. All experiments were repeated at least three times with at least three treated and three untreated plants per repeat. Letters indicate statistical significance (P 5 0.05) by one-way ANOVA (n = 6). Bar = 1 cm. Each box plot consists of borders corresponding to the 25th and 75th percentiles of the data, with data values included as points within the plot. The median is described by an inner, horizontal line and "X" corresponds to the mean. Whiskers describe the 1.5 x interquartile range of the data. Total flux represents the bioluminescent signal intensity determined within the ROI and is correlated with the amount of eATP present. L, local; S, systemic.

Downloaded from https://academic.oup.com/plphys/advance-article/doi/10.1093/plphys/kiac148/6555012 by University of Missouri-Columbia user on 06 June 2022

presented in Figure 1 demonstrate that wounding is followed by localized eATP accumulation, but that unlike ROS, the levels of eATP in systemic tissues do not change following wounding (at least within the time frame and detection limits of our method). The finding that ATP levels subsided at 20–30 min following wounding (Figure 1C) could suggest that ATP at the leaf surface undergoes degradation, by for example apyrases. To test whether ATP artificially applied to the leaf surface undergoes degradation, we applied a drop of 300 or 600 μM ATP to the surface of unwounded plants, waited 5 min, blotted the excess solution, and incubated the leaf for 5, 15, or 30 min. As shown in Figure 1D, eATP at the surface of unwounded leaves undergoes a time-dependent degradation process. In contrast, the same ATP concentrations kept in solution did not (Supplemental Figure S1). Based on these findings, we continued our analysis of eATP role in triggering systemic responses using stable ATP forms such as ATPγS and bzATP (Supplemental Figure S2; Chen et al., 2017; Pham et al., 2020; Duong et al., 2021).

Application of eATP to unwounded plants triggers the ROS wave

Because wounding was previously shown to trigger the ROS wave (Fichman et al., 2019), as well as to release ATP from cells (that becomes eATP; Figure 1; Kim et al., 2006; Roux, 2014), and the sensing of eATP by P2K1 was shown to trigger ROS production by RBOHD (Chen et al., 2017), we tested whether application of a stable form of eATP (bzATP; Chen et al., 2017; Pham et al., 2020; Duong et al., 2021) at different concentrations can trigger the ROS wave. As shown in Figure 2A, application of 0.1, 1, 50, or 300 μM bzATP to a single leaf of unwounded plants triggered the rapid accumulation of ROS in local and systemic leaves. This finding suggested that similar to different biotic and abiotic stresses such as heat, high light, or pathogen infection, applied to a local leaf (e.g. Fichman et al., 2019; Zandalinas et al., 2020a, 2020b), eATP application to a single leaf can trigger the ROS wave. The activation and propagation of the ROS wave by different abiotic and biotic stimuli is dependent on the function of RBOHD that is thought to drive the accumulation of ROS at the apoplast (Miller et al., 2009; Fichman et al., 2019). To test whether the local and systemic accumulation of ROS by eATP is also dependent on RBOHD, we applied 300 μM bzATP to wild-type (WT) and *rbohD* plants. As shown in Figure 2B, application of 300 μM bzATP to the *rbohD* mutant did not result in local and systemic ROS accumulation. The findings presented in Figure 2 suggest that eATP application to plants can trigger the ROS wave.

The activation of the ROS wave following application of eATP is dependent on the eATP receptor P2K

eATP is sensed in plant cells via the eATP receptors P2K1 and P2K2 leading to the activation of different metabolic and physiological responses (Choi et al., 2014; Chen et al., 2017; Pham et al., 2020). To test whether eATP application is triggering the ROS wave through the P2K pathway, we applied 300 μM bzATP to a single leaf of WT and P2K mutants (i.e. *p2k1-3*, *p2k2*, and *p2k1-3p2k2*; Choi et al., 2014; Chen et al., 2017; Pham et al., 2020) and measured local and systemic ROS accumulation. As shown in Figure 3, compared with WT, the local and systemic accumulation of ROS in response to 300 μM bzATP was completely blocked in the *p2k1-3*, *p2k2*, and *p2k1-3p2k2* mutants. This finding suggests that eATP can trigger the ROS wave via the P2K receptors, and that this response required both receptors to be functional.

The activation of the ROS wave following wounding is suppressed in mutants deficient in the eATP receptor P2K

The sensing of eATP by the eATP receptor protein P2K1 was previously shown to trigger ROS production in cells via phosphorylation of RBOHD (Chen et al., 2017). To test whether P2K1 is also involved in the activation of the ROS wave during wounding (Miller et al., 2009; Fichman et al., 2019; Fichman and Mittler, 2021), we measured local and systemic ROS accumulation in the *p2k1-3*, *p2k2*, and *p2k1-3p2k2* mutants. As shown in Figure 4, compared with WT, the accumulation of local and systemic ROS in the P2K mutants was suppressed following wounding of a local leaf. These finding suggest that the sensing of eATP during wounding plays an important role in triggering the ROS wave. The finding that in contrast to eATP application (Figure 3), the ROS wave was not completely suppressed in the P2K mutants following wounding (Figure 4) suggests, however, that additional wound-related signals, for example, Glu (Mousavi et al., 2013; Toyota et al., 2018; Shao et al., 2020), could also be involved in the triggering of the ROS wave following mechanical wounding. Indeed, the ROS wave was previously shown to be suppressed in the *glr3.3glr3.6* double mutant in response to wounding (Fichman and Mittler, 2021). The findings presented in Figures 3 and 4 suggest that both P2Ks are required for SWRs. One possible explanation is that P2K1 and P2K2 have complemented functions in different tissues, and that both are required for mediating systemic signals during wounding (somewhat akin to GLR3.3 and GLR3.6, or RBOHD and RBOHF, during wounding or high light stress, respectively; Nguyen et al., 2018; Zandalinas et al., 2020b).

The expression of wound- and ROS-response transcripts is suppressed in systemic leaves of mutants deficient in the eATP receptor P2K following local wounding

The ROS wave was previously shown to be required for systemic transcriptomic responses to local heat, high light, or mechanical stress treatments (Suzuki et al., 2013; Fichman and Mittler, 2020; Zandalinas et al., 2020a, 2020b; Fichman and Mittler, 2021). However, the role of eATP, P2Ks, and the ROS wave in triggering systemic transcriptomic responses to

Downloaded from https://academic.oup.com/plphys/advance-article/doi/10.1093/plphys/kiac148/6555012 by University of Missouri-Columbia user on 06 June 2022

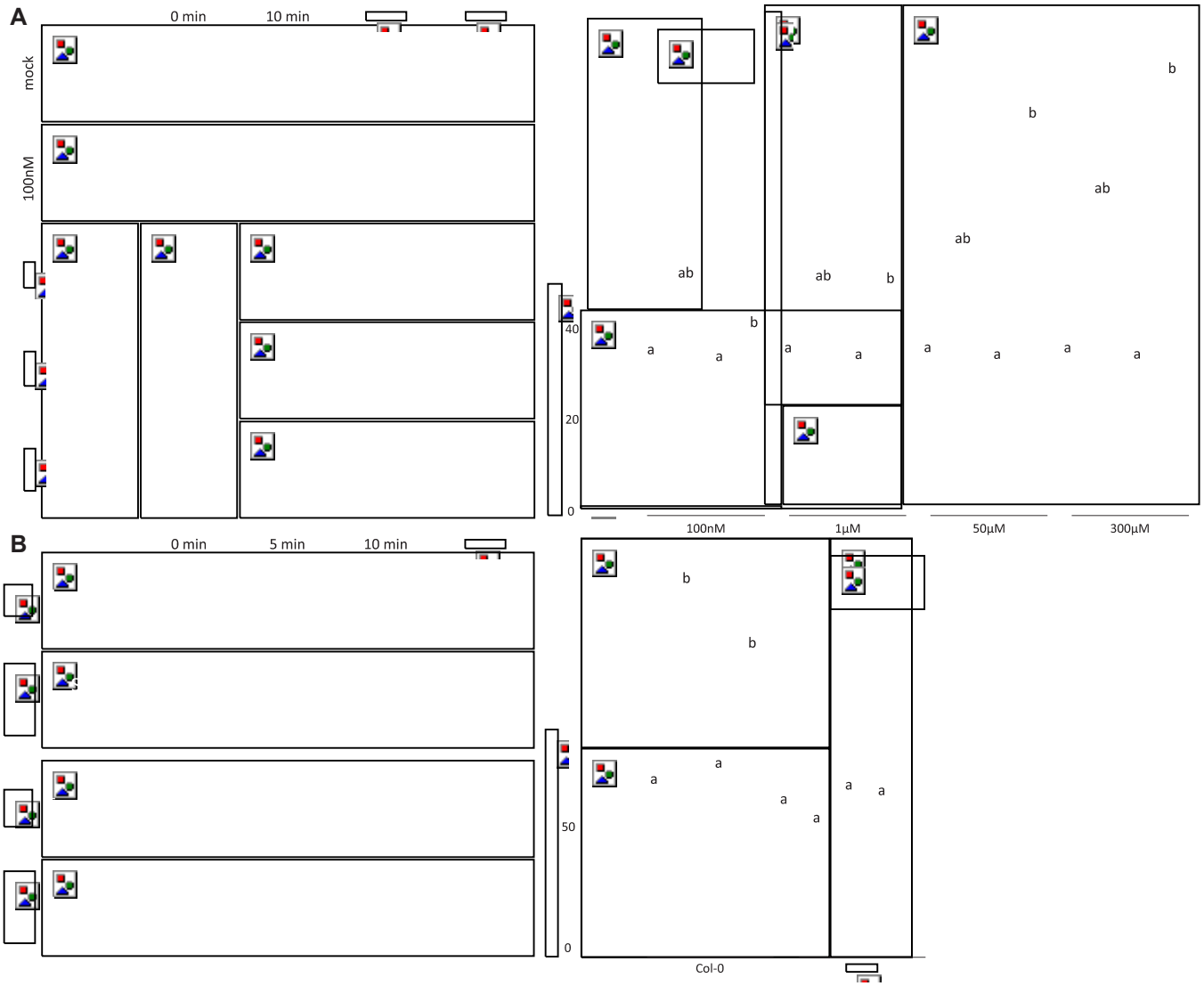

Figure 2 Application of eATP to unwounded plants triggers the ROS wave. A, Representative time-lapse images of whole-plant ROS levels (indicated by DCF oxidation) in Arabidopsis plants following the application of 0 (mock), 0.1, 1, 50, or 300 mM bcmeATP to a single leaf (local; L), along with statistical analysis of ROS levels in local and systemic (S) leaves of ATP or mock treated plants at 30-min following ATP application. B, Same as in (A), but for WT (Col-0) and *rbohD* plants treated on their local leaf with 0 (mock) or 300 mM bcmeATP. All experiments were repeated at least three times with at least three treated and three untreated plants per repeat. Letters indicate statistical significance ($P \leq 0.05$) by one-way ANOVA ($n = 6$). Bar = 1 cm. Each box plot consists of borders corresponding to the 25th and 75th percentiles of the data, with data values included as points within the plot. The median is described by an inner, horizontal line and "X" corresponds to the mean. Whiskers describe the 1.5 x interquartile range of the data. Letters represent a statistically significant difference corresponding to at least $P \leq 0.05$. L, local; S, systemic.

wounding is not clear. Because the ROS wave is suppressed following wounding in the P2K mutants (Figure 4), we tested whether this suppression is also affecting the expression of several wound- and ROS-response systemic transcripts (i.e. the zinc-finger proteins *ZAT10* and *ZAT12*, and the transcriptional regulator *WRKY40*; Suzuki et al., 2013; Zandalinas et al., 2019, 2020a, 2020b; Fichman and Mittler, 2021). As shown in Figure 5, compared with WT, the local and systemic expression of *ZAT10* and *WRKY40*, and the systemic expression of *ZAT12*, were suppressed in the *p2k1-3*, *p2k2*, and *p2k1-3p2k2* mutants following a local wounding treatment. This finding suggests that the sensing of eATP plays an important role not only in the triggering of the ROS wave following wounding, but also in the activation of some transcriptomic responses in systemic leaves. Because *ZAT12* expression is regulated via multiple signaling pathways (Davletova et al., 2005), it is possible that other wound-induced signal transduction pathways (e.g. redox, Glu, pH, and hormones; Vega-Muñoz et al., 2020) activate its expression in local leaves during wounding. In contrast, the systemic expression of *ZAT12* (Figure 5) is strictly dependent on the ROS wave (Miller et al., 2009).

Downloaded from https://academic.oup.com/plphys/advance-article/doi/10.1093/plphys/kiac148/6555012 by University of Missouri-Columbia user on 06 June 2022

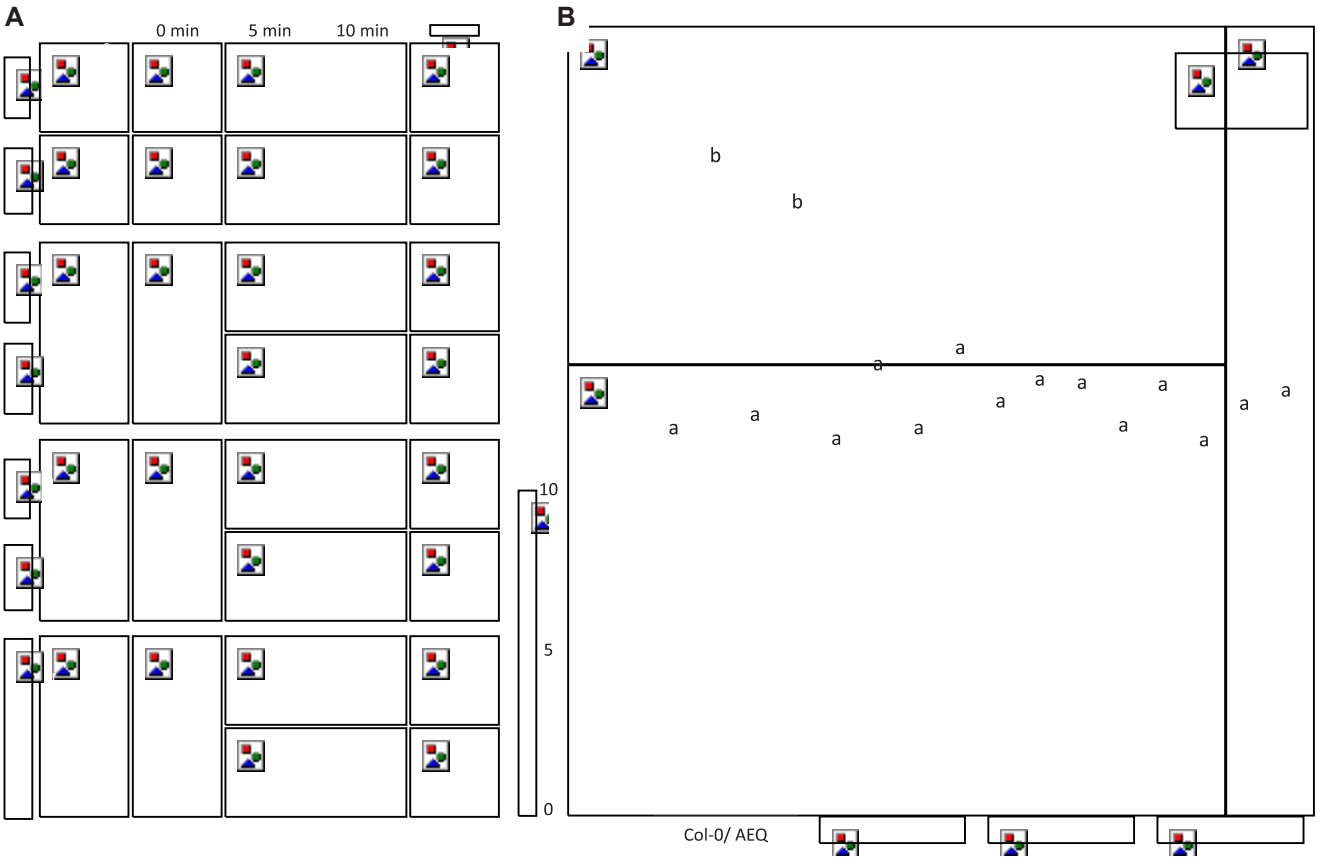

Figure 3 The activation of the ROS wave following application of eATP is dependent on the eATP receptors P2Ks. A, Representative time-lapse images of whole plant ROS levels (indicated by DCF oxidation) in WT (Col-0) and *p2k1-3*, *p2k2*, and *p2k1-3p2k2* plants following application of 0 (mock), or 300 mM bcmeATP to a single leaf (local; L). B, Statistical analysis of L and systemic (S) ROS levels in leaves of treated or mock untreated (on leaf L) WT and *p2k1-3*, *p2k2*, and *p2k1-3p2k2* mutant plants at 20 min following buffer/eATP application. All experiments were repeated at least three times with at least three treated and three untreated plants per repeat. Letters indicate statistical significance (P 5 0.05) by one-way ANOVA (n = 6). Bar = 1 cm. Each box plot consists of borders corresponding to the 25th and 75th percentiles of the data, with data values included as points within the plot. The median is described by an inner, horizontal line and "X" corresponds to the mean. Whiskers describe the 1.5 x interquartile range of the data.

Application of Glu, eATP, or eATP + Glu to unwounded plants triggers the ROS wave

Our findings that the ROS wave was not completely abolished in the P2K mutants following wounding (Figure 4) suggested that other wound-induced signals could be involved in triggering the ROS wave during wounding. To examine this question further, we first compared in side-by-side experiments the intensity of the ROS wave triggered by wounding to that triggered by the application of 300 1M bcmeATP. As shown in Figure 6A, wounding or eATP application induced comparable levels of the systemic ROS wave, with the levels induced by eATP being slightly lower. This finding suggested that eATP could be cooperating with other wound-induced signals, for example, Glu to induce the systemic ROS wave during wounding. To further test whether eATP and Glu could have a synergistic effect on the activation of the ROS wave, we applied eATP, Glu, or eATP + Glu to a local leaf and measured the local and systemic accumulation of ROS. As shown in Figure 6B, application of Glu, eATP, or eATP + Glu resulted in a similar systemic ROS accumulation response. Compared with eATP, application of Glu to a local leaf generated, however, a lower local ROS response. The findings presented in Figure 6 suggest that Glu or eATP can trigger the ROS wave during wounding, but that they likely trigger it via the same pathway.

Conclusions

The local wound response is a complex response that involves the activation of multiple signaling pathways. These include pathways responding to membrane depolarization, eATP, Glu, pH, ROS, and different plant hormones, including JA (e.g. Mousavi et al., 2013; Tripathi et al., 2017; Nguyen et al., 2018; Toyota et al., 2018; Farmer et al., 2020; Ikeuchi et al., 2020; Shao et al., 2020; Vega-Mu˜noz et al., 2020; Moore et al., 2021). While Glu, pH, and membrane depolarization were recently shown to trigger the SWR via GLR-triggered electric, calcium and ROS waves (Mousavi et al., 2013; Nguyen et al., 2018; Toyota et al., 2018; Shao et al., 2020; Fichman and Mittler, 2021; Figure 6B), the role of eATP in triggering SWR is not established. Our study reveals

Downloaded from https://academic.oup.com/plphys/advance-article/doi/10.1093/plphys/kiac148/6555012 by University of Missouri-Columbia user on 06 June 2022

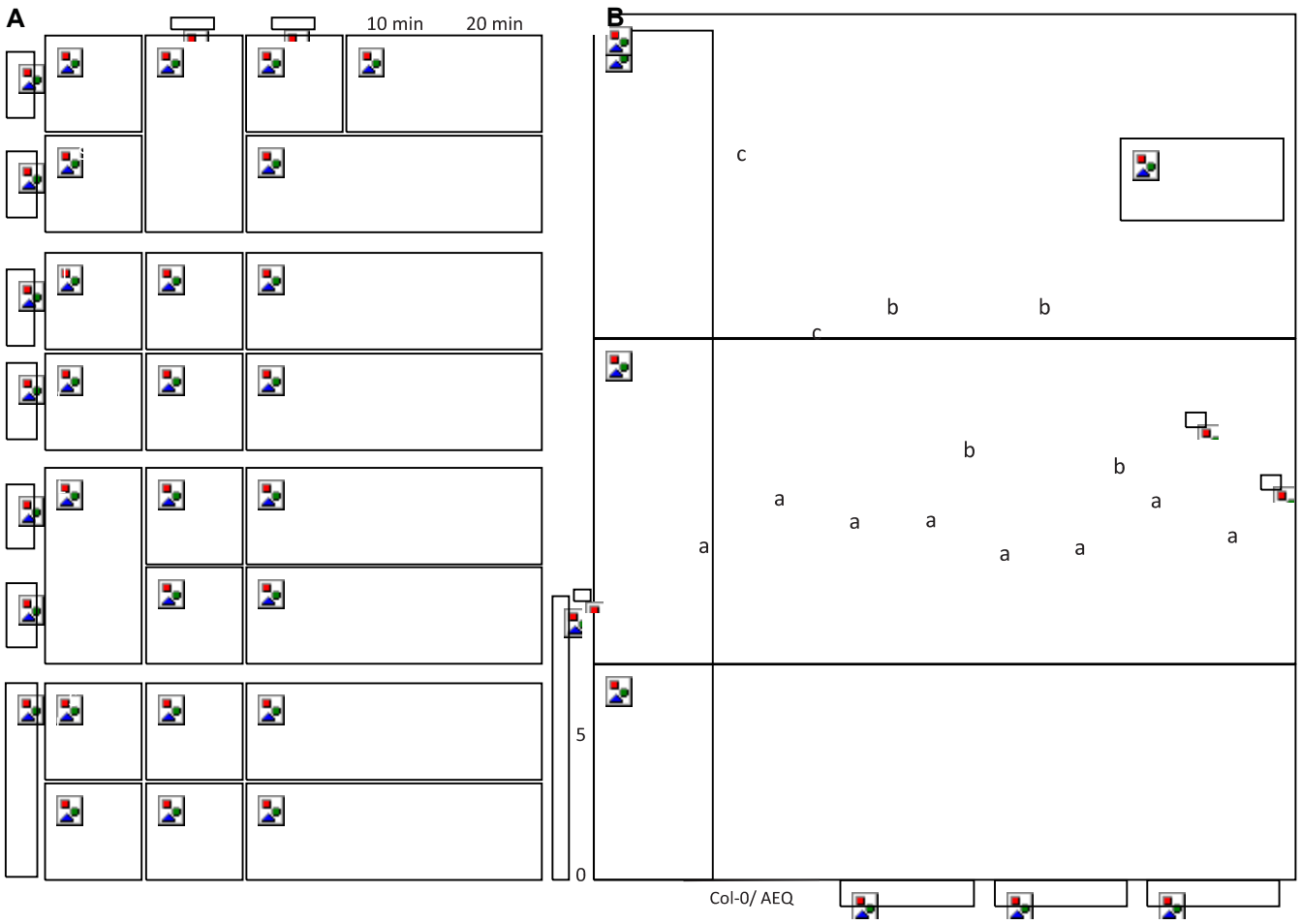

Figure 4 The activation of the ROS wave following wounding is suppressed in mutants deficient in the eATP receptors P2Ks. A, Representative time-lapse images of whole plant ROS levels (indicated by DCF oxidation) in WT (Col-0) and *p2k1-3*, *p2k2*, and *p2k1-3p2k2* plants following wounding of a single leaf (local; L). B, Statistical analysis of L and systemic (S) ROS levels in leaves of wounded or unwounded (on leaf L) WT and *p2k1-3*, *p2k2*, and *p2k1-3p2k2* mutant plants at 20 min following wounding. All experiments were repeated at least three times with at least three treated and three untreated plants per repeat. Letters indicate statistical significance (P 5 0.05) by one-way ANOVA (n = 6). Bar = 1 cm. Each box plot consists of borders corresponding to the 25th and 75th percentiles of the data, with data values included as points within the plot. The median is described by an inner, horizontal line and "X" corresponds to the mean. Whiskers describe the 1.5 x interquartile range of the data.

that during mechanical wounding eATP plays an important role in triggering the ROS wave and SWRs, and that eATP triggers these responses via a P2K and RBOHD dependent pathway (Chen et al., 2017; Figure 6C). However, because the ROS wave and the SWR are not completely blocked in the P2K mutants (Figures 4 and 5), it is likely that other pathways involved in SWR (e.g. the Glu-GLR pathway; Mousavi et al., 2013; Nguyen et al., 2018; Toyota et al., 2018; Shao et al., 2020; Figure 6B) could be playing a role in this response (Figure 6C). Further studies are therefore needed to determine how eATP is integrated with other wound-induced signal transduction pathways. For example, it would be interesting to test whether eATP application would trigger the ROS wave in the *glr3.3glr3.6* double mutant. In addition, because systemic signaling is mediated via distinct groups of cells in plants (e.g. phloem and xylem parenchyma cells; Nguyen et al., 2018; Zandalinas et al., 2020b; Zandalinas and Mittler, 2021), it would be interesting to examine whether there is a link between the function of P2K1 and P2K2 in inducing the ROS wave during wounding (Figure 4) and their expression in different plant tissues (similar to the studies described in Nguyen et al., 2018 and Zandalinas et al., 2020b, for GLR3.3GLR3.6 and RBOHD, respectively). When it comes to local and systemic ROS production during wounding, our findings that RBOHD is essential for ROS accumulation in response to eATP (Figure 2), as well as in response to wounding (Fichman and Mittler, 2021), suggests that RBOHD is a central integrator of wound-induced ROS associated signals (Figure 6C). RBOHD could, therefore, integrate eATP-activated P2K kinase activity, with GLR- and cyclic nucleotide-gated channel (CNGC)-driven calcium, and/or GLR- and CNGC-driven calcium-dependent kinase (CPK) activity (e.g. Dubiella et al., 2013) to trigger the ROS wave (Figure 6C). In future studies it would be interesting to find out whether the activation of the ROS wave during eATP application or wounding (Figures 3 and 4) is mediated via phosphorylation of RBOHD on amino acids S22 and T24 by P2K1, similar to the pathway proposed for P2K1 and

Downloaded from https://academic.oup.com/plphys/advance-article/doi/10.1093/plphys/kiac148/6555012 by University of Missouri-Columbia user on 06 June 2022

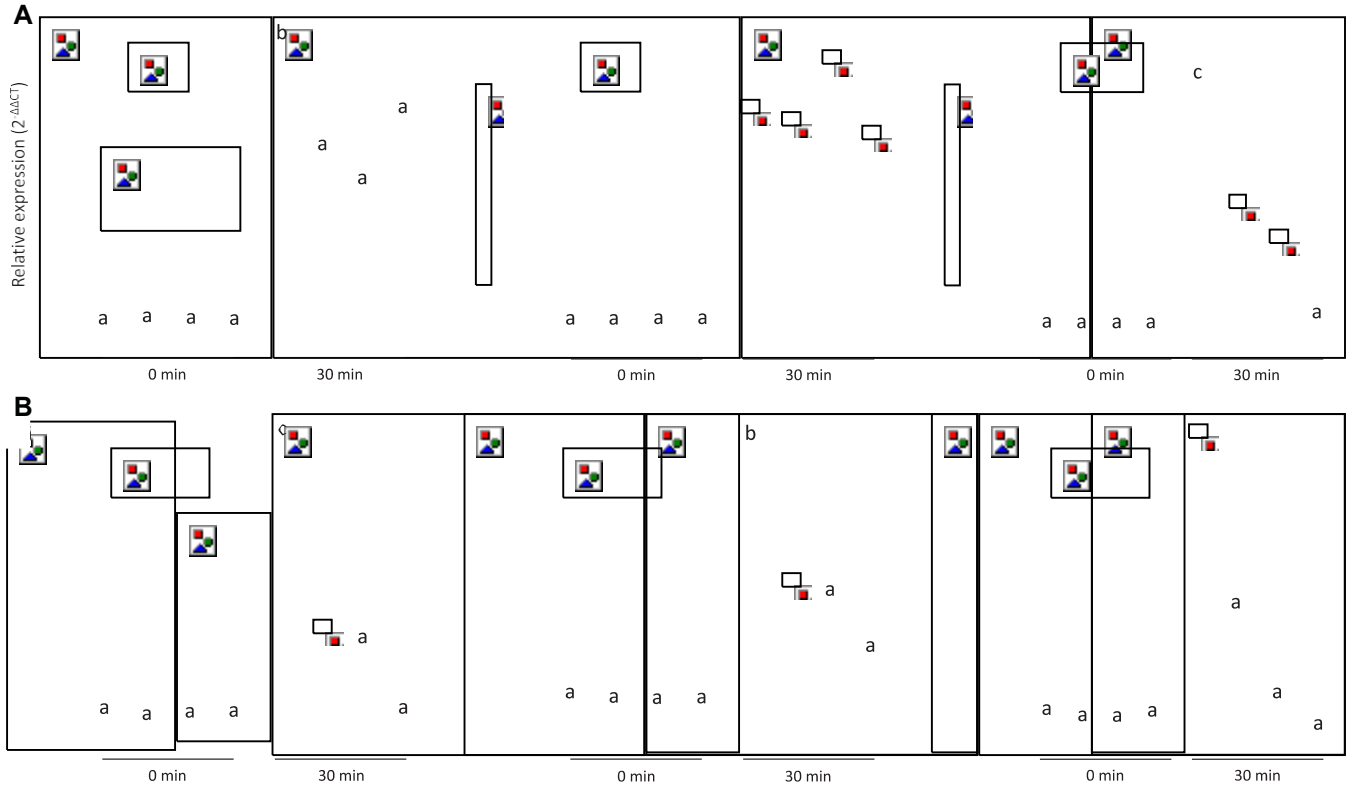

Figure 5 The expression of wound- and ROS-response transcripts is suppressed in systemic leaves of mutants deficient in the eATP receptors P2Ks following local wounding. A, T-qPCR analysis for *ZAT10*, *ZAT12*, and *WRKY40* steady-state transcript levels in local leaves of WT (Col-0) and *p2k1-3*, *p2k2*, and *p2k1-3p2k2* plants following wounding of a single leaf. B, Same as in (A), but for systemic leaves. Transcript expression is represented as the relative quantity (2^{-DDCT}) compared to an internal control (elongation factor 1a) in unwounded local tissue of WT (time 0). All experiments were repeated at least three times with at least three treated and three untreated plants per repeat. Letters indicate statistical significance ($P \leq 0.05$) by two-way ANOVA ($n = 6$). Each box plot consists of borders corresponding to the 25th and 75th percentiles of the data, with data values included as points within the plot. The median is described by an inner, horizontal line and "X" corresponds to the mean. Whiskers describe the 1.5× interquartile range of the data.

RBOHD function during stomatal regulation in response to bacterial pathogen infection (Chen et al., 2017).

Materials and methods

Plant materials, growth conditions, and stress treatments

Arabidopsis (*A. thaliana*) (Col-0) WT, *rbohD* (AT5G47910; Torres et al., 2002), and aequorin-expressing WT and *p2k1-3* (Choi et al., 2014; Chen et al., 2017; SALK_042209), *p2k2* (GK-777H06; Pham et al., 2020), and *p2k1p2k2* (SALK_042209/GK-777H06; Pham et al., 2020) plants were grown on peat pellets (Jiffy 7; Jiffy International, Kristiansand, Norway) for 4 weeks under controlled short-day conditions of 10-h-light/14-h-dark, 50 mmol $m^{-2}s^{-1}$, and 21°C ambient temperature. Wounding was applied to a single leaf by puncturing with 18 dressmaker pins simultaneously as described in Fichman et al. (2019). eATP was applied to a single leaf via submersion for 5 s in a dipping solution of 0, 0.1, 1, 50, or 300 mM bcmeATP, 300 mM ATP, or 300 mM ATPcS (Sigma-Aldrich Inc., St. Louis, MO, USA), 50 mM H_2DCFDA (Sigma-Aldrich Inc., St. Louis, MO, USA), and 2.67 mM $MgSO_4$ (Thermo Fisher Scientific, Waltham, MA, USA) in 0.1 mM EDTA, 0.05 M phosphate buffer, pH 7.4, 0.01% (v/v) Silwet L-77, as described in Kim et al. (2006) and Fichman et al. (2019). Due to its high stability, 300 mM bcmeATP was used for subsequent analysis of the ROS wave in different mutants, and comparisons to wounding or Glu application. Glu was applied to a single leaf via submersion for 5 s in a dipping solution of 100 mM L-Glutamic acid (Sigma-Aldrch, Inc., St. Louis, MO, USA), 50 mM H2DCFDA (Sigma-Aldrich Inc., St. Louis, MO, USA), 0.05 M phosphate buffer, pH 7.4, and 0.01% (v/v) Silwet L-77.

eATP imaging

To visualize eATP following wounding, plants were sprayed until leaf saturation and runoff with 1 mM luciferin (sodium salt; GOLD Biotechnology, Saint Louis, MO, USA; Miller et al., 2009), 10 mg/mL firefly luciferase (Promega, Madison, WI, USA), and 5 mM $MgCl_2$ in 0.5 M Tris–HCl, pH 7.5. A local leaf was then immediately wounded as described above. After an initial 5 min incubation period in darkness (to eliminate light-induced bioluminescent background), images of the resulting bioluminescence were acquired for 1 h using

Downloaded from https://academic.oup.com/plphys/advance-article/doi/10.1093/plphys/kiac148/6555012 by University of Missouri-Columbia user on 06 June 2022

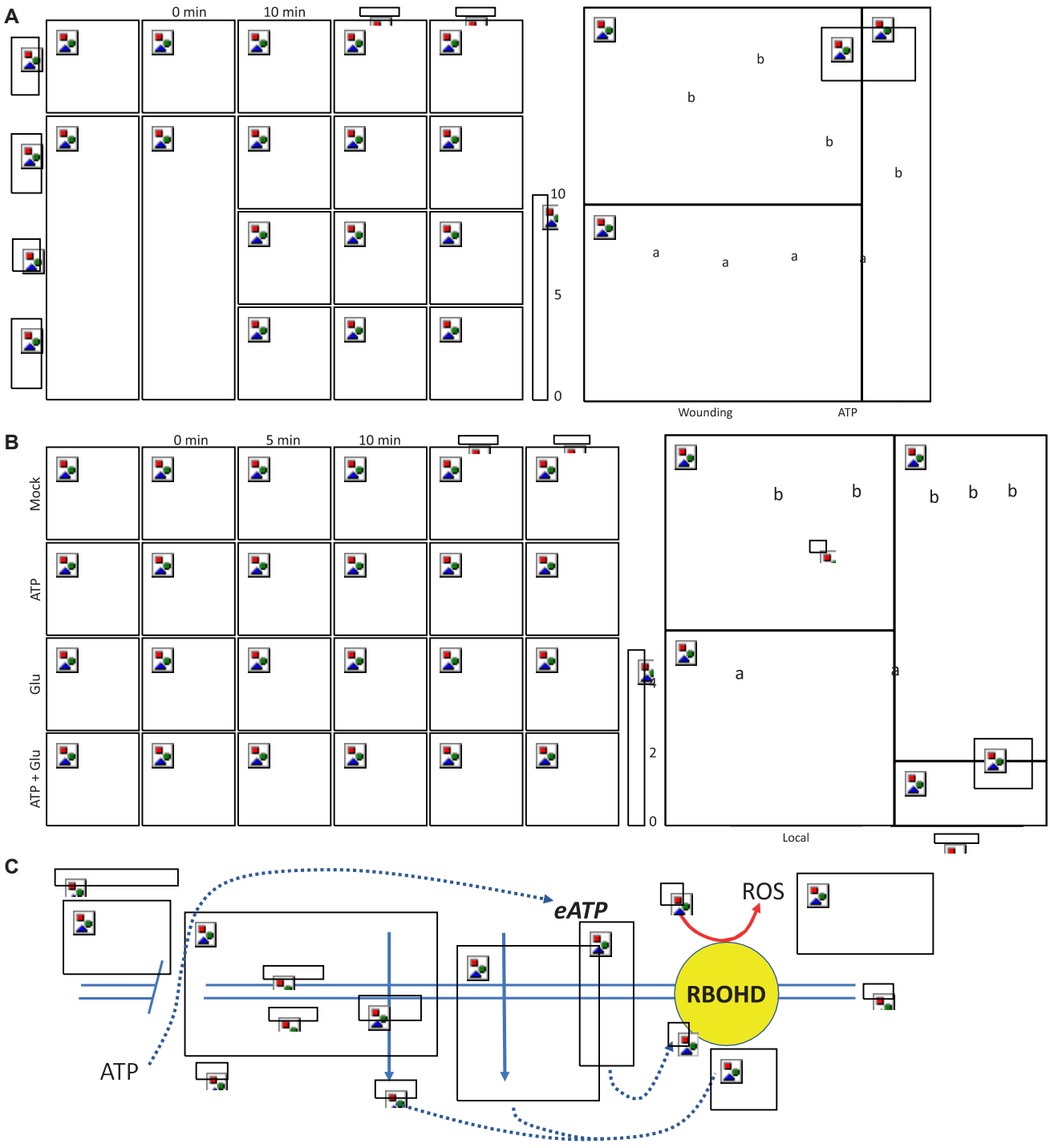

Figure 6 Side-by-side comparison between wounding and eATP application, as well as between Glu, eATP, or eATP + Glu application, and a model. A, Representative time-lapse images of whole-plant ROS levels (indicated by DCF oxidation) for a side-by-side comparison between the local (L) and systemic (S) ROS response of Arabidopsis plants to wounding or the application of 300 mM bcmeATP, along with statistical analysis of ROS levels in L and S leaves 30 min following eATP application or wounding. B, Representative time-lapse images of whole-plant ROS levels in Arabidopsis plants following the application of bcmeATP (300 mM), Glu (50 mM), or bcmeATP (300 mM) + Glu (50 mM) to a single leaf (L; buffer without ATP or Glu was applied to leaf L of mock untreated plants), along with statistical analysis of L and S ROS levels in leaves of treated or mock untreated (on leaf L) plants at 20 min following buffer/eATP/Glu/ATP + Glu application. All experiments were repeated at least three times with at least three treated and three untreated plants per repeat. Letters indicate statistical significance (P 5 0.05) by one-way ANOVA (n = 6). Bar = 1 cm. Each box plot consists of borders corresponding to the 25th and 75th percentiles of the data, with data values included as points within the plot. The median is described by an inner, horizontal line and "X" corresponds to the mean. Whiskers describe the 1.5 x interquartile range of the data. C, A hypothetical model depicting the proposed role of eATP in triggering the ROS wave during wounding. The sensing of eATP by P2Ks, as well as the sensing of Glu by GLRs is shown to trigger ROS production by RBOHD and initiate the ROS wave. ER, endoplasmic reticulum; P, phosphate; S, systemic.

Downloaded from https://academic.oup.com/plphys/advance-article/doi/10.1093/plphys/kiac148/6555012 by University of Missouri-Columbia user on 06 June 2022

the IVIS Lumina S5 system (PerkinElmer, Waltham, MA, USA) and analyzed using Living Image version 4.7.2 software as described in Fichman et al. (2019) and Zandalinas et al. (2020b). Quantification of bioluminescence in regions of interest was calculated using counts (photons/second) as described by Zandalinas et al. (2020b). Positive bioluminescent controls were performed by the application of a drop (10 µL) of ATP (10 mM; Sigma Aldrich Inc., St. Louis, M, USA) to a single leaf with no wounding. To quantify ATP levels following wounding, a standard curve for ATP levels was generated using a dilution series of ATP (Sigma-Aldrich Inc., St Louis, MO, USA) from 0 to 500 nM in a 96-well plate, mixed with 1 mM luciferin, 10 mg/mL firefly luciferase, 5 mM $MgCl_2$ in 0.5 M Tris–HCl, pH 7.5. The plate was placed side-by-side with wounded plants that were sprayed with 1 mM luciferin, 10 mg/mL firefly luciferase, 5 mM $MgCl_2$ in 0.5 M Tris–HCl, pH 7.5, and imaged for luciferase activity as described above. To determine the degradation rate of eATP applied to the leaf surface, a drop (10 µL) of ATP (0, 300, or 600 µM; Millipore-Sigma) was placed on a leaf. Following 5 min incubation the drop was blotted off the leaf surface using a sterile 3MM Whatman paper and the leaf was incubated for 5 more minutes. Plants were then sprayed with 1 mM luciferin, 10 mg/mL firefly luciferase, 5 mM $MgCl_2$ in 0.5 M Tris–HCl, pH 7.5, and imaged for luciferase activity as described above. All experiments were repeated at least three times with at least three biological repeats per treatment, each with 10–15 individual plants per genotype, per treatment.

ROS imaging

Whole-plant ROS accumulation was imaged and analyzed as described in Fichman et al. (2019). Plants were fumigated for 30 min with 50 mM H_2DCFDA (SigmaAldrich Inc., St. Louis, MO, USA) in 0.05 M phosphate buffer, pH 7.4, 0.01% (v/v) Silwet L-77 using a nebulizer (Punasi Direct, Hong Kong, China) within a glass enclosure to allow for uptake of the vaporized solution into the plants. Following fumigation, a single leaf was wounded or treated with eATP as described above and images of the resulting ROS wave were captured over 30 min using the IVIS Lumina S5 system (PerkinElmer, Waltham, MA, USA). Images were analyzed using Living Image version 4.7.2 and data analysis was performed by measuring radiant efficiency in regions of interest as described in Fichman et al. (2019). Accumulation of ROS compared to the 0-min time point was determined by subtracting the fluorescent signal of the initial time point (0-min) from the time point of interest. The 0-min time point was the initial image, which results in no signal being visualized due to fluorescence subtraction (Fichman et al., 2019). To ensure penetration of the H_2DCFDA dye into plants, controls were performed by fumigation with 0.3% (v/v) H_2O_2 for 10 min after 50 mM H_2DCFDA fumigation for 30 min and image acquisition in the IVIS Lumina S5 system (Fichman et al., 2019; Fichman and Mittler, 2020; Zandalinas et al., 2020b). All experiments were repeated at least three times with at least three biological repeats per treatment, each with 10–15 individual plants per genotype, per treatment.

Transcript expression analysis

Transcriptional responses of local and systemic leaves following wounding were analyzed at 0- and 30-min following wounding. Young systemic leaves located approximately 137.5° away from the sampled local leaf within the rosette were chosen for sampling. Plants wounded at a single leaf were allowed to incubate for 30 min following wounding prior to sampling of the local and systemic leaf. Four biological repeats for each treatment were used each with 12 technical repeats. RNA extraction was performed using Plant RNeasy kit (Qiagen, Hilden, Germany) as described by the manufacturer. Complementary DNA was synthesized from the quantified extracted RNA template (Primescript RT Reagent Kit; Takara Bio, Shiga, Japan). Reverse transcription-quantitative polymerase chain reaction (RT-qPCR) analysis of transcript expression was performed for genes *ZAT10* (AT5G59820), *ZAT12* (AT1G27730), and *WRKY40* (AT1G80840) using iQ SYBR Green supermix (Bio-Rad, Hercules, CA, USA) in the CFX Connect Real-Time PCR Detection System (Bio-Rad) as described in Fichman and Mittler (2021). *ELONGATION FACTOR 1A* served as the internal control to normalize relative gene expression across samples. Primer sequences used for each transcript are shown in Supplemental Table S1. Quantification of normalized relative gene expression (2^{-DDCT}) is presented as percent of control (with the unwounded local sample acting as the control).

Statistical analysis

Statistical analysis for all ROS and ATP imaging was performed with one-way analysis of Variance (ANOVA) followed by a Tukey post-hoc test. Two-way ANOVA followed by a Bonferroni test was performed for analysis of RT-qPCR experiments. Results are shown as box-and-whisker plots with borders corresponding to the 25th and 75th percentiles of the data. All data values are included as points within the plot, with a horizontal line corresponding to the median and "X" corresponding to the mean. Letters represent a statistically significant difference corresponding to at least $P \leq 0.05$.

Accession numbers

Sequence data from this article can be found in the GenBank/EMBL data libraries under accession numbers GLR 3.3 - NM_103438.3; GLR 3.6 - NM_115007.4; CNGC2 - NM_121545.5; CNGC6 - NM_001335878.1; P2K1 - NM_001085304.1; P2K2 - NM_114412.3; RBOHD - NM_124165.3; Zat10 - NM_102538.3; Zat12 - NM_125374.3; WRKY40 - NM_106732.4.

Supplemental data

The following materials are available in the online version of this article.

Downloaded from https://academic.oup.com/plphys/advance-article/doi/10.1093/plphys/kiac148/6555012 by University of Missouri-Columbia user on 06 June 2022

Supplemental Figure S1. Stability of ATP in solution.

Supplemental Figure S2. A comparison between the effects of ATP, ATPcS, and bcmeATP on the activation of the ROS wave.

Supplemental Table S1. Primers for transcript expression analysis via RT-qPCR.

Funding

This work was supported by funding from the National Science Foundation (IOS-2110017; IOS-1353886, MCB-1936590, and IOS-1932639), the Interdisciplinary Plant Group, the University of Missouri, the National Institute of General Medical Sciences of the National Institutes of Health (grant no. R01GM121445), the Next-Generation BioGreen 21 Program Systems and Synthetic Agrobiotech Center, Rural Development Administration, Republic of Korea (grant no. PJ01325403), and through the third call of the ERA-NET for Coordinating Action in Plant Sciences, with funding from the US National Science Foundation (IOS1826803).

Conflict of interest statement. None declared.

References

Chen D, Cao Y, Li H, Kim D, Ahsan N, Thelen J, Stacey G (2017) Extracellular ATP elicits DORN1-mediated RBOHD phosphorylation to regulate stomatal aperture. Nat Commun 8: 2265

Choi J, Tanaka K, Cao Y, Qi Y, Qiu J, Liang Y, Lee SY, Stacey G (2014) Identification of a plant receptor for extracellular ATP. Science 343: 290–294

Davletova S, Schlauch K, Coutu J, Mittler R (2005) The zinc-finger protein Zat12 plays a central role in reactive oxygen and abiotic stress signaling in Arabidopsis. Plant Physiol 139: 847–856

Dubiella U, Seybold H, Durian G, Komander E, Lassig R, Witte C-P, Schulze WX, Romeis T (2013) Calcium-dependent protein kinase/NADPH oxidase activation circuit is required for rapid defense signal propagation. Proc Natl Acad Sci USA 110: 8744–8749

Duong HN, Cho SH, Wang L, Pham AQ, Davies JM, Stacey G (2021) Cyclic nucleotide gated ion channel 6 is involved in extracellular ATP signaling and plant immunity. Plant J doi: 10.1111/tpj.15636

Farmer EE, Gao YQ, Lenzoni G, Wolfender J-L, Wu Q (2020) Wound- and mechanostimulated electrical signals control hormone responses. New Phytol 227: 1037–1050

Farmer EE, Goossens A (2019) Jasmonates: what ALLENE OXIDE SYNTHASE does for plants. J Exp Bot 70: 3373–3378

Farmer EE, Gasperini D, Acosta IF (2014) The squeeze cell hypothesis for the activation of jasmonate synthesis in response to wounding. New Phytol 204: 282–288

Fichman Y, Miller G, Mittler R (2019) Whole-plant live imaging of reactive oxygen species. Mol Plant 12: 1203–1210

Fichman Y, Mittler R (2021) Integration of electric, calcium, reactive oxygen species and hydraulic signals during rapid systemic signaling in plants. Plant J 107: 7–20

Fichman Y, Mittler R (2020) Rapid systemic signaling during abiotic and biotic stresses: is the ROS wave master of all trades? Plant J 102: 887–896

Ikeuchi M, Rymen B, Sugimoto K (2020) How do plants transduce wound signals to induce tissue repair and organ regeneration? Curr Opin Plant Biol 57: 72–77

Kim SY, Sivaguru M, Stacey G (2006) Extracellular ATP in plants. Visualization, localization, and analysis of physiological significance in growth and signaling. Plant Physiol 142: 984–992

Matthus E, Sun J, Wang L, Bhat MG, Mohammad-Sidik AB, Wilkins KA, Leblanc-Fournier N, Legu e V, Moulia B, Stacey G, et al. (2020) DORN1/P2K1 and purino-calcium signalling in plants: making waves with extracellular ATP. Ann Bot 124: 1227–1242

Miller G, Schlauch K, Tam R, Cortes D, Torres MA, Shulaev V, Dangl JL, Mittler R (2009) The plant NADPH oxidase RBOHD mediates rapid systemic signaling in response to diverse stimuli. Sci Signal 2: ra45 doi:10.1126/scisignal.2000448

Monshausen GB, Bibikova TN, Weisenseel MH, Gilroy S (2009) Ca^{2+} regulates reactive oxygen species production and pH during mechanosensing in Arabidopsis roots. Plant Cell 21: 2341–2356

Moore BM, Lee YS, Wang P, Azodi C, Grotewold E, Shiu S-H (2021) Modeling temporal and hormonal regulation of plant transcriptional response to wounding. Plant Cell 34: 867–888

Mousavi SAR, Chauvin A, Pascaud F, Kellenberger S, Farmer EE (2013) GLUTAMATE RECEPTOR-LIKE genes mediate leaf-to-leaf wound signalling. Nature 500: 422–426

Nguyen CT, Kurenda A, Stolz S, Ch etelat A, Farmer EE (2018) Identification of cell populations necessary for leaf-to-leaf electrical signaling in a wounded plant. Proc Natl Acad Sci USA 115: 10178–10183

Pham AQ, Cho SH, Nguyen CT, Stacey G (2020) Arabidopsis lectin receptor kinase P2K2 is a second plant receptor for extracellular ATP and contributes to innate immunity1. Plant Physiol 183: 1364–1375

Roux SJ (2014) A start point for extracellular nucleotide signaling. Mol Plant 7: 937–938

Shao Q, Gao Q, Lhamo D, Zhang H, Luan S (2020) Two glutamate- and pH-regulated Ca2 + channels are required for systemic wound signaling in Arabidopsis. Sci Signal 13: eaba1453

Song CJ, Steinebrunner I, Wang XZ, Stout SC, Roux SJ (2006) Extracellular ATP induces the accumulation of superoxide via NADPH oxidases in Arabidopsis. Plant Physiol 140: 1222–1232

Suzuki N, Miller G, Salazar C, Mondal HA, Shulaev E, Cortes DF, Shuman JL, Luo X, Shah J, Schlauch K, et al. (2013) Temporal–spatial interaction between reactive oxygen species and abscisic acid regulates rapid systemic acclimation in plants. Plant Cell 25: 3553–3569

Tian W, Wang C, Gao Q, Li L, Luan S (2020) Calcium spikes, waves and oscillations in plant development and biotic interactions. Nat Plants 6: 750–759

Torres MA, Dangl JL, Jones JDG (2002) Arabidopsis gp91phox homologues AtrbohD and AtrbohF are required for accumulation of reactive oxygen intermediates in the plant defense response. Proc Natl Acad Sci USA 99: 517–522

Toyota M, Spencer D, Sawai-Toyota S, Jiaqi W, Zhang T, Koo AJ, Howe GA, Gilroy S (2018) Glutamate triggers long-distance, calcium-based plant defense signaling. Science 361: 1112–1115

Tripathi D, Zhang T, Koo AJ, Stacey G, Tanaka K (2017) Extracellular ATP acts on jasmonate signaling to reinforce plant defense. Plant Physiol 176: 511–523

Vega-Mun~oz I, Duran-Flores D, Ferna´ndez-Ferna´ndez ÁD, Heyman J, Ritter A, Stael S (2020) Breaking bad news: dynamic molecular mechanisms of wound response in plants. Front Plant Sci 11: 1959

Walker-Simmons M, Holla¨nder-Czytko H, Andersen JK, Ryan CA (1984) Wound signals in plants: a systemic plant wound signal alters plasma membrane integrity. Proc Natl Acad Sci USA 81: 3737–3741

Wang L, Ning Y, Sun J, Wilkins KA, Matthus E, McNelly RE, Dark A, Rubio L, Moeder W, Yoshioka K, et al.. (2022) *Arabidopsis thaliana* CYCLIC NUCLEOTIDE-GATED CHANNEL2 mediates extracellular ATP signal transduction in root epidermis. New Phytol 234: 412–421 doi: 10.1111/nph.17987. Epub ahead of print. PMID: 35075689

Downloaded from https://academic.oup.com/plphys/advance-article/doi/10.1093/plphys/kiac148/6555012 by University of Missouri-Columbia user on 06 June 2022

Zandalinas SI, Fichman Y, Devireddy AR, Sengupta S, Azad RK, Mittler R (2020a) Systemic signaling during abiotic stress combination in plants. Proc Natl Acad Sci USA 117: 13810–13820

Zandalinas SI, Fichman Y, Mittler R (2020b) Vascular bundles mediate systemic reactive oxygen signaling during light stress. Plant Cell 32: 3425–3435

Zandalinas SI, Mittler R (2021) Vascular and nonvascular transmission of systemic reactive oxygen signals during wounding and heat stress. Plant Physiol 186: 1721–1733

Zandalinas SI, Sengupta S, Burks D, Azad RK, Mittler R (2019) Identification and characterization of a core set of ROS wave-associated transcripts involved in the systemic acquired acclimation response of Arabidopsis to excess light. Plant J 98: 126–141

Downloaded from https://academic.oup.com/plphys/advance-article/doi/10.1093/plphys/kiac148/6555012 by University of Missouri-Columbia user on 06 June 2022